Volume 10, Issue 05, May 2024,
Publish Date: 14-05-2024
Doi https://doi.org/10.55640/ijmsdh-10-05-07

International Journal of Medical Science and Dental Health (Open Access)

IN-SILICO STUDY OF DESTABILIZING ALZHEIMER'S AB42 PROTOFIBRILS WITH CURCUMIN

ABDUL FARIS HUSSEIN[1], HAMED.H. KHAMEES[1], ALI ABDULMAWJOOD MOHAMMED[2], SAIF ALI MOHAMMED HUSSEIN[1], MOHAMMAD ABDALJABBAR AHMED[1], ARKAN SAAD MOHAMMED RAOOF[3]

[1]MedicaL laboratory Techniques, Dijlah University College
[2]College of Science, Mustansiriyah University, Baghdad, Iraq
[3]Al-Nahrain University, College of Engineering, Biomedical Engineering Department

ABSTRACT

Aggregation of amyloid beta (Aβ) peptides leads to formation of fibrilar, soluble oligomers, and their deposition is a key event in progression of Alzheimer's disease (AD). Recent experimental studies of (Curcumin) showed\ significant Aβ aggregation inhibition, but its molecular mechanism is not yet clear. Hence, the present study aims at exploring the underlying mechanism of destabilization and inhibition of aggregation of the Aβ protofibril by Curcumin at the molecular level. Molecular docking analysis shows that Curcumin binds to chain E of the Aβ protofibril through hydrogen bonding interactions. Comparative molecular dynamics simulations depict the binding of Curcumin at the edge of chain E, and its partially inserted conformation at the hydrophobic core destabilizes the Aβ protofibril. Its binding causes loss of hydrophobic contacts, leading to a partial opening of tightly packed β-sheet protofibrils. The hydration effect of salt bridge between the amino group of Lys28 and the oxygen atom of Curcumin contributes in destabilization of Aβ protofibrils. Binding free energy calculations of Curcumin and the Aβ protofibril showed that van der Waals interactions are dominant over the others. Thus, our results revealed that Curcumin interacts mainly with the hydrophobic core along with positively charged residues of the Aβ protofibril for effective destabilization. Thus, this structural information could be useful to design new inhibitors to control the aggregation of Aβ protofibrils in AD patients.

INTRODUCTION

Alzheimer's disease (AD) is the most common cause of dementia and is characterized by the accumulation of amyloid plaques, with the main constituent being the amyloid-beta peptide (Aβ). It is estimated that 24 million victims are suffering from AD worldwide, and there is no effective pharmacological treatment available at present (1). Relative abundance of Aβ in an AD brain is essential for disease development; however, the mechanism of Aβ mediated neurotoxicity is less obvious. Several possible mechanisms have been proposed (2) Normally, Aβ42 exists as disordered monomer; however,

in AD patients, it eventually undergoes conformational transition into aggregation-prone β-conformation that self-assembles into protofibril and fibrillar structure (3). The studies that address the folding of non-native conformation into thermodynamically stable native conformation will be helpful to predict the factors that dictate conformation transition in the misfolded proteins (4, 5). The therapeutic strategies targeting Aβ42 self-assembly can be divided into 3 major categories: (1) reducing the formation of Aβ42, (2) preventing Aβ42 aggregation by stabilizing native conformation of Aβ42 or to destabilize the aggregation prone β- sheet conformation, and (3) and clearance of aggregates from the brain.(6) Considering recent research that oligomers, protofibril, are the toxic species associated with AD, they become interesting targets for experimental as well as theoretical investigations.(3,7) The various anti-aggregation agents that include small molecules,(8) nanoparticles,9 peptides,(10) and degrading enzymes11 have been recently reported. In the search of Aβ42 aggregation inhibitors, the role of small organic molecules against Aβ42 fibrillation is considered crucial. Curcumin is a natural compound derived from the herb turmeric (6). Recent research has focused on its mechanisms of action by which it can modulate AD progression. This review examines the efficacy of curcumin to treat AD. It describes the pathophysiology of AD, current pharmacotherapies for AD, and the problems with existing therapies. Then, the review delineates the major mechanisms of action by which curcumin acts on the multi-faceted disease process of AD. Finally, the challenges associated with curcumin treatment are discussed and directions for future research are outlined.

MATERIAL AND METHODS

Preformed Aβ17-42 protofibrils with and without Curcumin molecules.

Two systems were simulated: Aβ17-42 protofibrils in the absence and presence of Curcumin molecules, denoted by respectively Aβ and Aβ+ Curcumin. According to previous MD simulation studies (7, 8), we choose a pentamer as a protofibril model in our MD simulations. The initial coordinates of the pentameric Aβ17-42 protofibril was taken from the solid-state NMR derived Aβ17-42 fibril structure determined by Luhrs et al. (PDB ID: 2BEG). In this fibril model, residues 1-16 are ignored due to their disordered nature and residues 17-42 form an in-register parallel β-strand-turn-β-strand structure13. In our study, the N-terminal (residues 18-26) and the C-terminal (residues 31-41) β-sheets are respectively named as β1 and β2 regions, which are linked by a turn spanning residues 27-30, as shown in Fig. 1A. The initial structure of the Dih molecule was taken from the ChemSpider. The chemical structure of a Curcumin molecule and the initial state of the Aβ+ Curcumin system are shown in Fig. 1B and 1C, respectively.

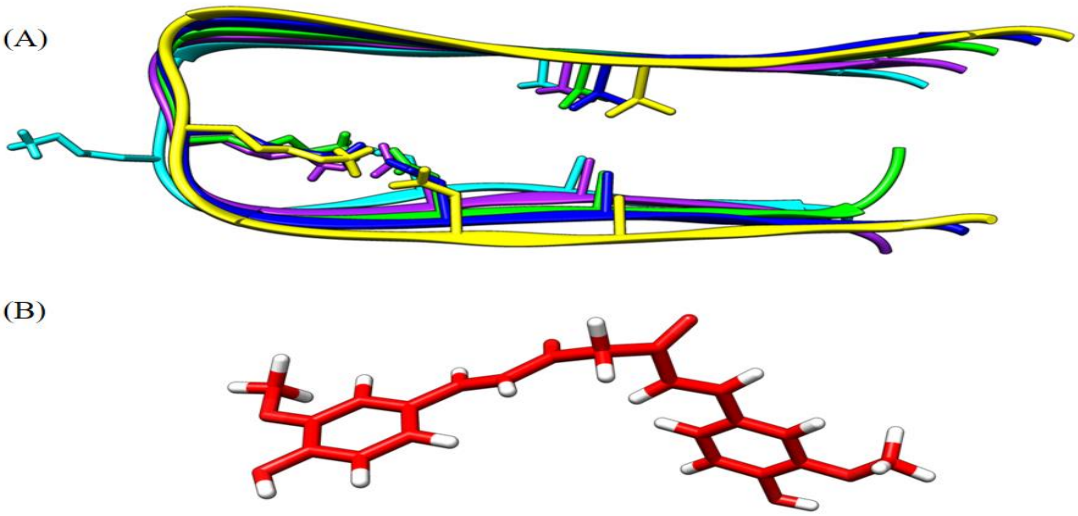

Figure1: (A) *(Solution structure of A protofibril (PDB ID: 2BEG). (B) 3D Structure of Curcumin.)*

Molecular Docking

The docking simulation of protofibril Aβ was assembled, conducted, and analysed using AutoDock with the clustering algorithm. AutoDock 4.2 with Lamarckian Genetic Algorithm was used to execute the molecular docking experiments (LGA) (Permanne, Adessi 2002, Kaur, Goyal 2020). The simulation details are listed in Table 1.

Table 1 *(Lowest Two binding energy out of 50 runs of each Aβ Monomer- PMB and Aβ protofibril- PMB.)*

Set No.	Docked systems	Auto Dock Binding energy in kcal/mol	Inhibition constant mM
Set I	Aβ protofibril- PMB	-1.68	58.27
	Aβ protofibril- PMB	-1.26	118.56
Set II	Aβ Monomer- PMB	-2.44	16.35
	Aβ Monomer- PMB	-1.51	78.85

We used blind docking to identify potential binding mechanisms of oleocanthal to Aβ protofibril. The population size was set to 150 people such that 100 conformations could be generated during 27000 generations and 25000000 energy evaluations. The Aβ42 protofibril– curcumin complex have been kept in a cubic box with dimensions 87 Å × 59 Å × 76 Å 37. The Aβ42 peptide in the two systems was protonated based on the physiological pH (7.4). Population size, conformations grid centre were set to X = 0.238 Y = 0.189 Z =-6.69. Lamarckian Genetic Algorithm (LGA), which combines global search (Genetic Algorithm) and local search (Solis and Wets algorithm), was chosen from among the stochastic search algorithms available in the AutoDock suite. Hydrophobic interactions between Aβ42 protofibril residues and compounds were seen using UCSF Chimera.

Molecular dynamic simulation

In the present study, two systems were constructed (Aβ42 protofibril, docked complex of Aβ42 protofibril with curcumin). The two systems were protonated based on the physiological pH (7.4). The N-terminal and C-terminal of the Aβ42 peptide were kept protonated and deprotonated, respectively. The two systems were solvated by using the simple point charge (SPC) water model(8) and were neutralized by adding sufficient Na+ ions as per the literature.(9) The particle mesh Ewald (PME) method was used to calculate the long-range electrostatic interactions, and the cutoff for short-range van der Waals interactions was kept at 1.0 nm.(10) The LINCS algorithm with an integration time step of 2 fs was used to constraint the bond lengths.(11) The equilibration of the systems was done under the NVT ensemble for 1 ns at 300 K followed by the second phase of equilibration under the NPT ensemble for 1 ns at 1 bar. In all MD simulations, the temperature was maintained at 300 K using a modified Berendsen thermostat (12) and the pressure was maintained at 1 bar using a Parrinello−Rahman barostat.(13) the two systems were simulated for a time period of 100 ns, and the trajectories were saved at every 10 ps time interval. After the completion of simulations, GROMACS tools along with Discovery studio (14) UCSF Chimera (13) were used for the analysis of the trajectories. The MD ensemble was clustered using a root-mean-square deviation (RMSD)-based cluster analysis over backbone atoms with a cutoff of 0.20 nm. (12) The RMSD and root-mean-square fluctuation (RMSF) analyses were performed using GROMACS tool "gmx rms", "gmx rmsf" respectively, to elucidate the structural stability of the Aβ42 peptide in all the four systems. The tertiary contacts between the residues were determined using the GROMACS tool "gmx mdmat". The repeat simulations with different initial velocities have been performed for the Aβ42 monomer and Aβ42.

Table 2: *(Backbone RMSD, RMSF, and Radius of gyration (nm ± S.D) values for all systems.)*

System	RMSD	RMSF
Aβ protofibril	2.8 ± 0.01	0.11± 0.04
Aβ protofibril + Curcumin	4.3 ± 0.04	0.1 ± 0.02

Table 2. *(Backbone RMSD values of each chain (Å ± S.D) for a system of Aβ protofibril.)*

System	Chain A	Chain B	Chain C	Chain D	Chain E	Overall
1.Aβ protofibril + Curcumin 100 ns	3.53±0.2	3.5±0.2	3.51±0.4	2.7±0.7	6.2±0.8	4.38±0.4
1.Aβ + protofibril 100 ns	3.41±0.2	2.87±0.2	2.86±0.1	2.75±0.19	3.04 ±40	2.88±0.13

RESULTS AND DISCUSSION

Elucidation of the binding modes, key interactions using molecular docking:

To elucidate the binding modes of Curcumin and its fluorinated analogues with Aβ42 protofibril, the molecular docking studies were performed Fig 2A. Ligand efficiency, in addition to weak interactions, is a useful term to identify lead molecule among ligands, and it is reported that the good binders usually have −0.35 or lower values of ligand efficiency.28. The hydrophobic interactions such as Phe 19 (A), Ala 21 (A), Gly 25 (A) Mainly observed for binding of Polymyxin at terminal side for chain A of Aβ protofibril. the data summarized in Table 1 indicate that ligand efficiency value lies near the standard value. The binding energy of Curcumin with Aβ42 protofibril is noted to be −10.26. The 2D protein-ligand interaction maps were generated using discovery studio and hydrophobic contacts between Aβ42 protofibril residues and Curcumin is shown in Figure 2B.

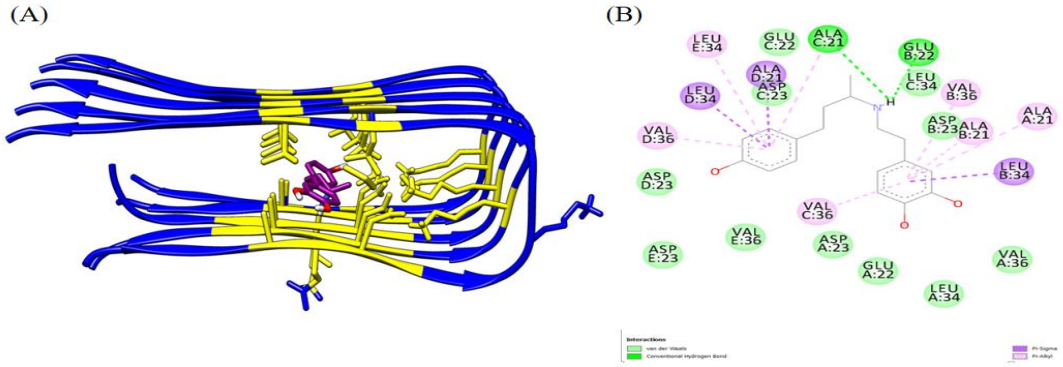

Figure2: (A) *(Possible binding mode of Curcumin to AβP and residues involved in binding shown in stick (purple), (B) 2D plot of Docking interaction between Curcumin and AβP.)*

Curcumin molecules destabilize Aβ17-42 protofibrils by mostly disrupting β1 and turn

Regions:

To evaluate the structural effects of Curcumin on the Aβ protofibril, MD simulation of blind docked and docked complexes was performed and evaluated on the basis of backbone rmsd, and rmsf of the Aβ protofibril (chains A−E). Interaction of Curcumin Hydrophobic core of Aβ protofibril causes increase in rmsd of the pentamer from 2.8 Å (protofibril alone) to 4.3 (Figure 2A). Similarly, the rmsd of each chain of the pentamer was found to fluctuate in the range of 2.8−3.4 Å (Table 3 Figures 3B). Comparing this with the control (Figures3A). Change in conformation of chain E was observed because of totaly insertion of Curcumin, causing fluctuations in amino acids of the Aβ protofibril (Figure 3 E, F). This trend of conformational change is slightly followed in a similar fashion by other chains to a lesser extent. The overall rmsf results show that Curcumin induces more flexibility near the Cterminal region (β-2 Leu17−Ser26) and loop (bend) region (Asn27−Ala30) of the protofibril rmsf fluctuates more in the presence of Curcumin with 0.17 and 0.15 nm, respectively, in the blind docked complex (Figure 3B).

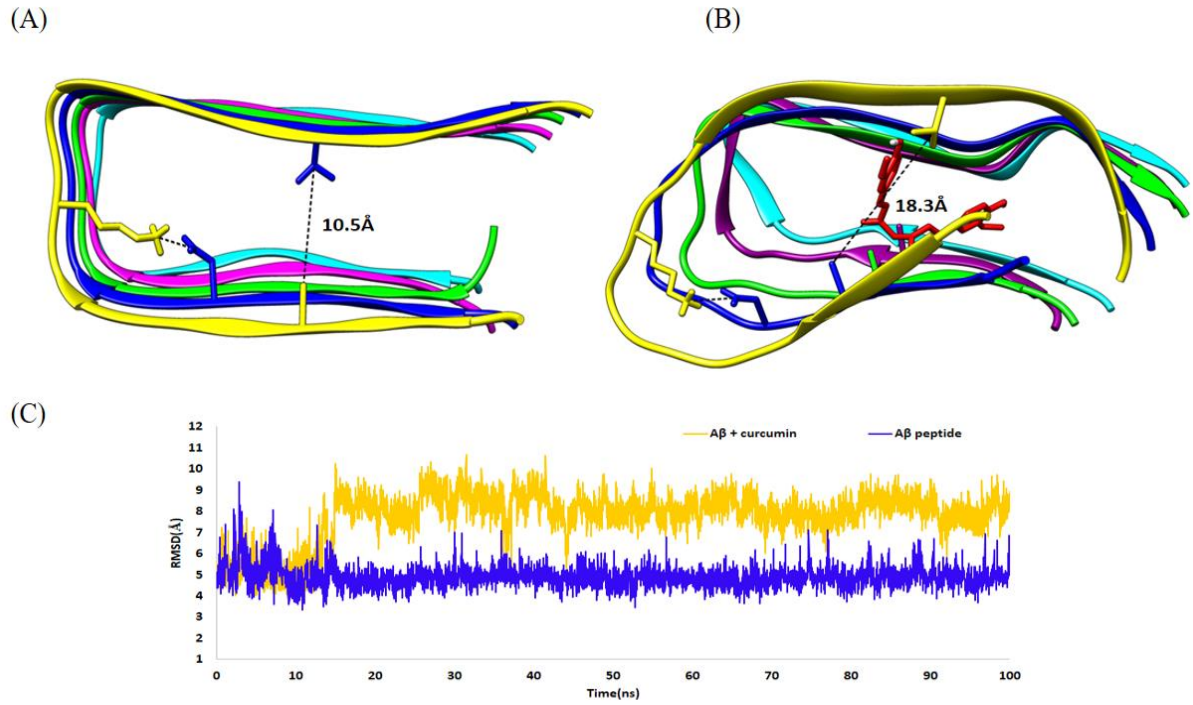

Figure3. (A) *(The snapshot displays the stability of the Ala21-Val36 and Asp23-Lys28 (salt bridge) of AβP in absent of Curcumin, (D) The snapshot displays disruption of a salt bridge at the turn region and Ala21-Val36 distance of AβP in presence of Curcumin (C)RMSD of backbone AβP (Blue) and AβP-Curcumin (orange))*

Table 3. *(Average interchain Ala21-Val36 distance (Å ± S.D) for all systems)*

Set	Chain AB	Chain BC	Chain CD	Chain DE	Overall
1.Aβ protofibril 100 ns	4.87±0.50	5.06±0.85	4.35±1.34	5.60±1.86	4.49±1.02
2.Aβ+ Curcumin l -docked 100ns	5.86±0.4	7.57±0.9	11.86±1.69	14.07±2.06	8.88±1.0

Destabilization of the Aβ Protofibril by Curcumin Peptides:

Entire inserted Curcumin at the edge of chain A (system Aβ+ Curcumin) shows slight destabilization in chains E and D (Figure 4A, B). It was further confirmed in simulations with the Aβ+ Curcumin -docked complex of both blind. The rmsd profiles of the Aβ+ Curcumin complex from docking show that chain E and chain D in the Aβ protofibril deviate more as compared to other chains (Figures 3B, F). This Entyre inserted conformation of Curcumin shows destabilizing effect similar to earlier studies. (14) The interchain distance between Ala21 and Val36 is indicative of compactness between two sheets. This

average interchain distance in the absence of an inhibitor is 5.24 ± 1.02 Å (set I-2) because of strong hydrophobic contacts in between two β-sheets specifically at residues Ala21–Ile32, which provides a stable secondary structure (β-sheet) to the Aβ protofibril (Figure S1). Simulation of the Aβ+RR-AFC-docked complex from blind as well as semiflexible docking shows that partial insertion of RR-AFC resulted into loss of hydrophobic contacts between two β-sheets, which has resulted in an increase in the average interchain distance between Ala21 and Val36 to 13.23 Å in a blind docked complex (set III 1-2) as compared to the control Aβ protofibril (Figure 3D). The interchain distance between Ala21 and Val36 for the semiflexible docked complex was found to be 6.40 Å (Figure 3D, set IV-3).

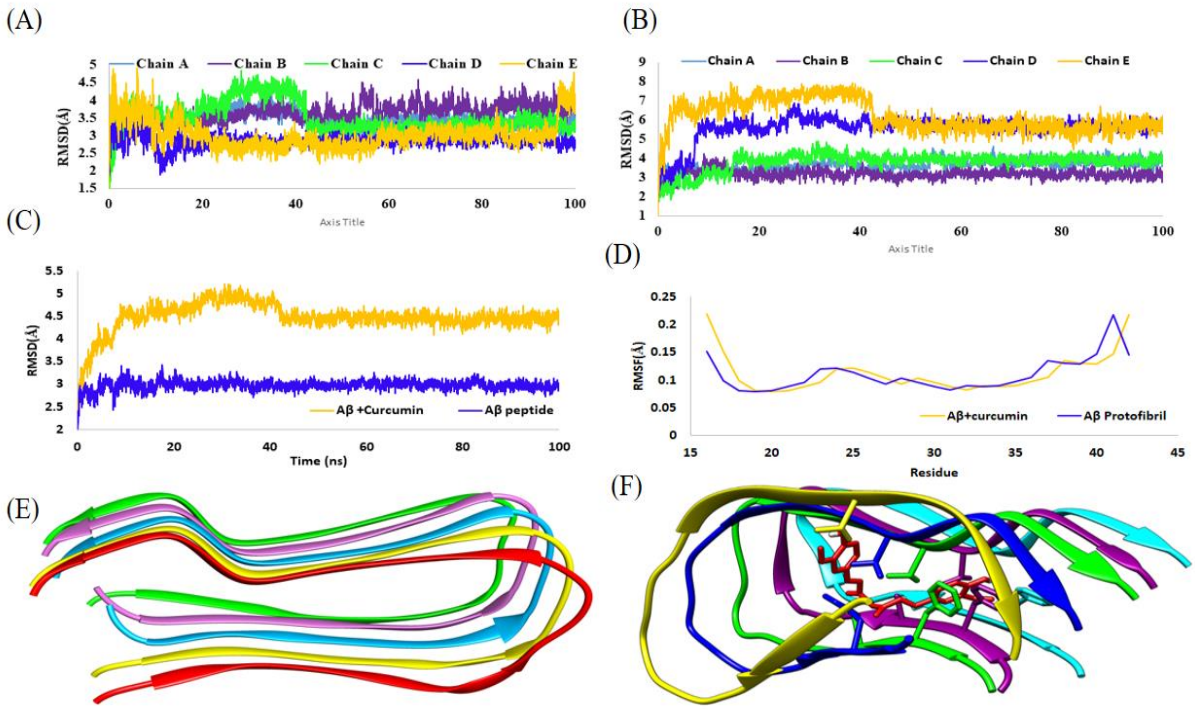

Figure 4: *(A) (Root-mean-squire-deviation (RMSD) of each chain (A-E) of AβP in absence of Curcumin, (B) RMSD of each chain (A-E) of AβP in presence of Curcumin (C) RMSD of backbone AβP (Blue) and AβP-Curcumin (orange) (D) Root-mean-square-fluctuation (RMSF) of Backbone. (E) normal structure of AβP in apsent of Curcumin (F) destabilized structure of AβP in present of Curcumin)*

CONCLUSION

In this study, we observed that Curcumin inhibits AβP oligomerization by establishing interactions with structural areas important in the formation of the antiparallel β-strand of the AβP oligomer. Blind docking of Curcumin investigated molecular interactions, revealing the presence of hydrogen bonding and Alkyl interactions between Curcumin and the Aβ protofibril. The AβP+ Curcumin and Aβ systems show that the oleocanthal molecule has a strong disruptive effect on the AβP. Curcumin molecules can damage both intra-chain and inter-chain Asp23-Lys28 salt bridges, which is essential for fibril stability, according to salt bridge investigations. Due to the actions of Curcumin on the hydrophobic groove of AβP, there will increase in the average interchain distance between Ala21 and Val36 which indicates

loss of compactness between two sheets. Binding to the C-terminal hydrophobic groove has a minor impact on the structures.

REFERENCES

1. Sonawane, K., Barale, S. S., Dhanavade, M. J., Waghmare, S. R., Nadaf, N. H., Kamble, S. A., ... & Naik, N. M. (2020). Homology modeling and docking studies of TMPRSS2 with experimentally known inhibitors Camostat mesylate. Nafamostat and Bromhexine hydrochloride to control SARS-Coronavirus-2.
2. Yassmine Chebaro, Ping Jiang, Tong Zang, Yuguang Mu, Phuong H. Nguyen, Normand Mousseau, and Philippe Derreumaux The Journal of Physical Chemistry B **2012** 116 (29), 8412-8422 DOI: 10.1021/jp2118778
3. Sonawane, K. D., Barale, S. S., Dhanavade, M. J., Waghmare, S. R., Nadaf, N. H., Kamble, S. A., ... & More, V. B. (2021). Structural insights and inhibition mechanism of TMPRSS2 by experimentally known inhibitors Camostat mesylate, Nafamostat and Bromhexine hydrochloride to control SARS-coronavirus-2: A molecular modeling approach. Informatics in medicine unlocked, 24, 100597.
4. Dah Ihm Kim, Ki Hoon Lee, Amr Ahmed Gabr, Gee Euhn Choi, Jun Sung Kim, So Hee Ko, Ho Jae Han, Aβ-Induced Drp1 phosphorylation through Akt activation promotes excessive mitochondrial fission leading to neuronal apoptosis, Biochimica et Biophysica Acta (BBA) - Molecular Cell Research, Volume 1863, Issue 11, doi.org/10.1016/j.bbamcr.2016.09.003
5. Mohammed, Z. J., Sharba, M. M., & Mohammed, A. A. (2022). The effect of cigarette smoking on haematological parameters in healthy college students in the capital, baghdad. European Journal of Molecular & Clinical Medicine.
6. Mohammed, A. A., Barale, S. S., Kamble, S. A., Paymal, S. B., & Sonawane, K. D. (2023). Molecular insights into the inhibition of early stages of Aβ peptide aggregation and destabilization of Alzheimer's Aβ protofibril by dipeptide D-Trp-Aib: A molecular modelling approach. International Journal of Biological Macromolecules, 242, 124880.
7. Al-Azzawi, M. A., Maftool, A. J., Al-Shimary, A. A., & Mohammed, A. A. (2023). A Comprehensive Review of Vitamin D3: Metabolism, Functions, and Clinical Implications. International Journal of Medical Science and Dental Health, 9(12), 37-46.
8. MacLeod, R., Hillert, E. K., Cameron, R. T., & Baillie, G. S. (2015). The role and therapeutic targeting of α-, β- and γ-secretase in Alzheimer's disease. Future science OA, 1(3), FSO11.
9. Mohammed, A. A., Mahmoud, H. Q., & Mhana, R. S. (2023). Advances in the diagnosis and management of breast cancer: a systematic review. World, 2(6).
10. Metaxas A, Kempf SJ. Neurofibrillary tangles in Alzheimer's disease: elucidation of the molecular mechanism by immunohistochemistry and tau protein phospho-proteomics. Neural Regen Res. 2016 Oct;11(10):1579-1581.
11. Mahmoud, H. Q., Mhana, R. S., & Mohammed, A. A. (2024). Therapeutic options and management approach on thalassemia an overview. International Journal of Medical Science and Dental Health, 10(01), 17-28.
12. O'Brien RJ, Wong PC. Amyloid precursor protein processing and Alzheimer's disease. Annu Rev Neurosci. 2011; 34:185-204.

13. Mohammed, A. A., & Sonawane, K. D. (2022). Destabilizing Alzheimer's Aβ42 protofibrils with oleocanthal: In-silico approach. BIOINFOLET-A Quarterly Journal of Life Sciences, 19(3), 288-295.
14. Permanne, B., Adessi, C., Saborio, G. P., Fraga, S., Frossard, M. J., Van Dorpe, J., Dewachter, I., Banks, W.A., Van Leuven, F. and Soto, C. (2002). Reduction of amyloid load and cerebral damage in transgenic mouse model of Alzheimer's disease by treatment with a β-sheet breaker peptide. The FASEB Journal, 16(8), 860-862.
15. Rajmohan R, Reddy PH. Amyloid-Beta and Phosphorylated Tau Accumulations Cause Abnormalities at Synapses of Alzheimer's disease Neurons. J Alzheimers Dis. 2017;57(4):975-999.
16. Kamble, S. A., Barale, S. S., Mohammed, A. A., Paymal, S. B., Naik, N. M., & Sonawane, K. D. (2024). Structural insights into the potential binding sites of Cathepsin D using molecular modelling techniques. Amino Acids, 56(1), 33.
17. Saini, R. K., Shuaib, S., & Goyal, B. (2017). Molecular insights into Aβ42 protofibril destabilization with a fluorinated compound D744: A molecular dynamics simulation study. Journal of Molecular Recognition, 30(12), e2656.
18. Stelzma, R.A., Schnitzlein, H.N., Murtaghf, R., 1995. An English translation of Alzheimer's 1907 paper “übereineeigenartigeErkrankung der Hirnrinde”. Clin. Anat. 8, 429–431.
19. Wang, ZX., Tan, L., Liu, J. et al. The Essential Role of Soluble Aβ Oligomers in Alzheimer’s Disease. Mol Neurobiol 53, 1905–1924 (2016).
20. Yang F et al.: Curcumin inhibits formation of amyloid oligomers and fibrils, binds plaques, and reduces amyloid in vivo. J Biol Chem 2005, 280:5892-5901.
21. Al-Karawi, A. S., Abdullah, A. M., Abdulraziq, M. S., Alubadi, A. E., Ajmi, R. N., & Ati, E. M. (2023). THE ENVIRONMENTAL REALITY OF DESERTIFICATION IN IRAQ/2022: A REVIEW ARTICLE. Open Access Repository, 9(6), 226-234.
22. Abdullah, A. M., Al-Karawi, A. S., Aswad, O. A. K., Alubadi, A. E., Ati, E. M., & Ajmi, R. N. (2023). Natural Reserves and Sustainable Development of AL-Tayeb Reserve/South Iraq: A Review Article. Global Scientific Review, 16, 29-37.
23. Al-Jindeel, T. J., Al-Karawi, A. S., Kready, H. O., & Mohammed, M. (2021). Prevalence of COVID-19 virus infection in asymptomatic volunteers in Baghdad city/Iraq during 2021. International Journal of Health Sciences, 6(S2), 5524-5530.
24. Al-Jandeel, T. J., Al-Karawi, A. S., Abdulrazzaq, O. I., & Tareq, S. (2023). An Evaluation of Laboratory Tests for COVID-19 Infection in Patients Residing in the Baghdad-Iraq. International Journal of Chemical and Biochemical Sciences, 23(1).
25. Al-Dahbi, A. M., Fadhel, A. N., & Hussein, S. A. M. (2009). Histological and Immunological Study of Daily Supplement of Aqueous extract of Thymus vulgaris Leaf in Mice Challenged with Vibrio alginolyticus.
26. Hussein, L. K. A. A Study on Isolation, Identification and the Distribution of Clostridium Species from Iraqi Soil Samples Lubna Kamil Abdul Hussein1, Saif Ali Mohammed Hussein, and Ali Hussein Alwan3.